Available online at www.sciencedirect.com
SCIENCE DIRECT®
ELSEVIER
European Journal of Mechanics B/Fluids 23 (2004) 519–533
EUROPEAN JOURNAL OF MECHANICS B/FLUIDS

Boundary layer development after a region of three-dimensional separated flow

C. Cao, P.E. Hancock *

Fluids Research Centre, School of Engineering, University of Surrey, Guildford, Surrey, GU2 7XH, UK

Received 10 February 2003; received in revised form 25 June 2003; accepted 30 October 2003

Abstract

The development of the boundary layer flow down stream of a region of three-dimensional turbulent separated flow has been investigated using hot-wire anemometry and pulsed-wire anemometry for wall shear stress. The flow, generated by means of a 'v-shaped' separation line, was set up so as to generate a central region of fully three-dimensional flow, bounded on each side by the degenerate case of spanwise-invariant flow, which is closely related to two-dimensional co-planar flow. The flow developing in the central region has fundamentally different features from that after a region of two-dimensional separated flow. A bulge in the boundary layer, generated in the separated flow, has a strong wake-like characteristic that sits very persistently in the outer part of the layer, its shape and relative size changing little in ~ 25 reattachment length scales. The Reynolds stresses in this bulge region, driven by the mean velocity gradient of the wake-like flow, are very much larger than the normal levels in the boundary layer or in the developing region downstream of a two-dimensional separation. The inner layer that lies beneath the bulge is subjected to a high level of non-shear-stress-containing motion, the normal stresses being much higher than the shear stress which exhibits a constant level in the inner layer despite much higher levels further out.

Keywords: Boundary layer development; Three-dimensional separated flow

1. Introduction

In many instances of practical concern a boundary layer flow has developed from a region of reattached separated flow, the latter having itself developed from some form of boundary layer flow. It is well established that turbulent flows often take not only a considerable distance to recover from a region of distortion but that the recovery is frequently non-monotonic. In general terms this behaviour arises because turbulence structure is sensitive to the imposition of 'extra' rates of mean strain, such as that caused by streamline curvature or divergence, and the imposition of a large disturbance imposes large changes in turbulence structure which in turn take a considerable distance (or time) to return to a 'normal' state. Castro and Epik [1] (hereafter denoted CE) noted that the term 'development' rather than 'recovery' or 'relaxation' is more appropriate because there is often no upstream turbulent boundary layer. Fernholz [2] distinguishes between weak and strong separated flows, in which the reverse flow is respectively weak and strong, and where a weak reverse flow interacts little with the separating boundary layer, while a strong reverse flow interacts strongly.

Numerous experiments show the inner layer of a boundary layer, when assessed from the mean velocity scaled on inner layer variables (y, u_τ, ν), to be resilient to changes in the outer layer, unexpectedly so in some respects (Bradshaw [3]). The classical justification is in part that the inner-layer length scale is small compared with the outer-layer scale, from which it is inferred that the inner-layer motion remains more readily in equilibrium. However, as is also well known, other quantities such as the

* Corresponding author.
E-mail address: p.hancock@surrey.ac.uk (P.E. Hancock).

0997-7546/$ – see front matter
doi:10.1016/j.euromechflu.2003.10.016

Reynolds stresses are much less resilient. In Townsend's concept of 'inactive motion' part of the inner-layer motion is driven by the outer-layer turbulence, scaling on outer-layer rather than inner-layer scales. The outer layer imposes lateral motions in the inner layer that do not contribute significantly to the Reynolds shear stress because the associated wall-normal velocity fluctuations are small compared with those of the inner-layer active motion. Consequently, the Reynolds stresses do not scale on the wall shear stress, though these lateral motions do not significantly affect the mean velocity in the inner layer. A similar effect is seen when free-stream turbulence is present, where the persistence of an inner layer conforming to an unchanged inner layer logarithmic law is argued on the basis that free-stream turbulence is like perturbed outer-layer turbulence (Hancock and Bradshaw [4]).

The turbulence in the outer part of a separated flow is much like that of a mixing layer and therefore very much more intense than it is in a canonical turbulent boundary layer. In qualitative terms at least the development downstream of reattachment must be that of an outer flow with mixing-layer like structures that change and decay in strength, beneath which a boundary-layer like flow must develop as an internal layer. As yet unresolved questions concern the development of this layer. Bradshaw and Wong [5] concluded that the inner layer structure developed the canonical form more quickly than the outer layer, whereas CE argue that the inner layer develops no more quickly than the outer layer which essentially determines the overall rate of development of the whole flow. However, although they analyse the behaviour of the inner layer in terms of free-stream turbulence imposed by the outer flow, drawing on the measurements of Hancock and Bradshaw [4], they do not make it clear whether the non-canonical structure can be attributed to inactive-type motions. Moreover, they do not present turbulence quantities in inner-layer scaling. In contrast, Song et al. [6] argue that the inner layer develops more rapidly and recovers normal boundary layer characteristics before the outer layer. However, they do so on the basis of an unconventional scaling for the inner layer, based on the work of DeGraaf and Eaton [7], where the scaling velocity is the geometric mean of the friction velocity and the free-stream velocity. In conventional scaling the Reynolds stress levels in the inner layer were still higher by the last station than they are in the canonical inner layer. Their flow was formed from a separating turbulent boundary layer which had a thickness comparable with the bubble length, whereas the bubble of CE was formed from a thin laminar layer. Turbulence levels are substantially higher in the latter case, and so some difference in rates of development would not be surprising.

Most detailed experimental studies of the development downstream of a separated region have, like those cited above and most studies of separated flow, been made in flows that are nominally two-dimensional and co-planar (where the term co-planar refers to planes of mean streamlines perpendicular to the invariant direction). Some studies have been made in axi-symmetric (unswirled) flow so as to avoid 'end effects' (e.g., Kalter and Fernholz [8]). Three-dimensional separated flows are considerably more complex than two-dimensional flow – which, though a crucial stepping stone for understanding, arise relatively rarely in practice – and are much less well understood as a consequence. An approach employed in recent studies (e.g., Hardman and Hancock [9]) has been to set up flows which on the one hand are fully three-dimensional but on the other are related to two-dimensional (co-planar) flow. This has been achieved here by means of a doubly-swept separation line, as illustrated in Fig. 1(b), where the flow formed near the centre-line is fully three-dimensional, while that formed sufficiently far to the sides has the property of spanwise invariance (provided end effects are small enough). The degree of sweep controls the degree of three-dimensionality in the central region and, what is more, the degree of general three-dimensionality varies with lateral position. Spanwise-invariant flows are, by definition, two-dimensional, but are not co-planar except in the special case of an unswept separation line. At least for moderate sweep angles, of less than about $\sim 40^\circ$ (Kaltenbach [10]), spanwise-invariant flows are not very different from the corresponding unswept flow once an axis system aligned with the separation line is used (Hancock and McCluskey [11]). Although, so far, this strategy has been used only in the study of sharp-edged separation there appears to be no reason why the same idea should not be used for systematic study of smooth-wall separated flows.

The present measurements show that the developing flow has an outer region exhibiting (axisymmetric) wake-like characteristics that sits above an underlying developing boundary layer, which necessarily has characteristics of a three-dimensional boundary layer, but which is otherwise not fundamentally different from that for two-dimensional co-planar flow. This wake-like region is very persistent, and the flow as a whole is therefore fundamentally different from that for two-dimensional co-planar flow; studies of the latter will *not* contain key physical features of the flow after certain regions of three-dimensional flow, therefore. Some features seen in the present flow resemble boundary layer flows with imbedded longitudinal vortices, such as that studied by Mehta and Bradshaw [12], though the streamwise vorticity there was much stronger than the very weak vorticity of the same sense (upwards in the centre) here.

Although not reported here, extensive comparisons were made between the developing layer downstream of spanwise-invariant, swept separation bubbles and that for two-dimensional co-planar (i.e., unswept) flow. These will be presented in due course, but as the differences are quite undramatic the emphasis of the present paper is on the fully three-dimensional flow.

2. Experimental techniques

The separated flows were generated at the leading edge of a bluff thick plate, made of aluminium of tooling plate quality, 8.1 mm thick, and made in two parts. The main part, of length 1.2 m, provided an unswept leading edge, and short leading edge pieces smoothly aligned at the junction provided singly and doubly swept separation lines, as shown in Fig. 1. Most of the measurements were made with sweep angles of 25° and ±25° (singly- and doubly-swept, respectively). The plate was mounted on the horizontal centre-plane of the wind tunnel working section, of width 600 mm and height 300 mm, and overall length of 2 m. The plate thickness was chosen so as to give adequate width in terms of size of the separated flow region (the distance to attachment), that is, wide enough to give regions of spanwise-invariant flow either side of the central region of the double-swept case. A laterally-sliding roof arrangement, driven by a stepper motor, and moveable roof panels allowed probes to be moved over the whole of the working section. Streamwise and vertical probe movements were also controlled by stepper motors, where the streamwise motion was allowed by means of a slot in the sliding roof, sealed either side of the probe support by means of a brush. The traverse mechanism itself was constructed from Parker slides driven by precision lead screws with a position resolution as fine as 0.001 mm. Measurements were made between x/X_r of 2 and 25, and at lateral positions of $Z = 0, \pm 10, \pm 25, \pm 32.5, \pm 40, \pm 50, \pm 60, \pm 75, \pm 100, \pm 150$ and ±200 mm, typically. Here, X_r, the distance to reattachment in the spanwise-invariant region, measured in the streamwise direction, was 48 mm. The axis system is described in Section 3. Unless otherwise stated, dimensional spatial co-ordinates are in mm.

X_r was measured by means of a two-tube differential pressure probe (Castro and Fackrell [13]), which has always been found to give good agreement with the pulsed-wire wall shear stress probe. For the unswept flow X_r was 5.2 plate thicknesses, which is very close to the length given by Cherry at al. [14] for the blockage of these experiments. (Earlier, unpublished, experiments in this wind tunnel, where the bubble length had been measured on both upper and lower surfaces, had also shown the free-stream flow to be at negligibly small incidence.)

Conventional hot-wire anemometry techniques were used for all the velocity measurements. Modified standard Dantec single-wire (P11) and cross-wire (P51) probe types were used: the wire lengths and diameter were nominally 0.5 mm and 2.5 μm, respectively, the prongs of the probes having been moved closer together and slightly reduced in diameter at the tips. Some cross-wire measurements were made with further modified probes having wire angles of ±60°, instead of the standard ±45°, but these probes were not used for the measurements presented here as the intensities at these stations were not high enough to necessitate their use. The streamwise velocity and moment fluctuations are from the single-wire measurements. The probes were driven by standard bridges operating at an overheat ratio of 0.7, and the output digitally processed via 16-bit ADC's under the control of data acquisition and control software written in LabView. The probes were calibrated statically according to $E^2 = E_0^2 + BU^n$, where E and U are respectively bridge voltage and velocity, and the other terms are calibration constants. Calibrations were carried out automatically and frequently enough to minimize any effects of drift. E_0 and B were corrected for temperature changes and n, typically 0.45, was adjusted to give best fit. The cross-wire measurements were made using the effective-angle method Bradshaw [15] for wire angle.

A pulsed-wire wall shear stress probe was used to make independent measurements of shear stress, since it could not be assumed that the inner layer mean flow would conform to the standard form. Once calibrated the probe provides in principle a direct measurement of mean and fluctuating shear stress. Calibration was made against Preston tubes (Patel [16]) in a standard turbulent boundary layer formed on the plate but with a gently-rounded leaded edge piece, upon which a transition trip was fixed, placed at the front. Three tubes of differing diameter were used as a check for self-consistency and accuracy. The pulsed-wire-probe calibration was of the usual form, namely $\tau = A + B(1/T) + C(1/T^2) + D(1/T^3)$, where T is the elapsed time and τ the wall stress. The probe could only be located in instrumentation plugs at discrete positions on the plate centre line (at 100, 200, 300 and 500 mm along the main, i.e., unswept, plate).

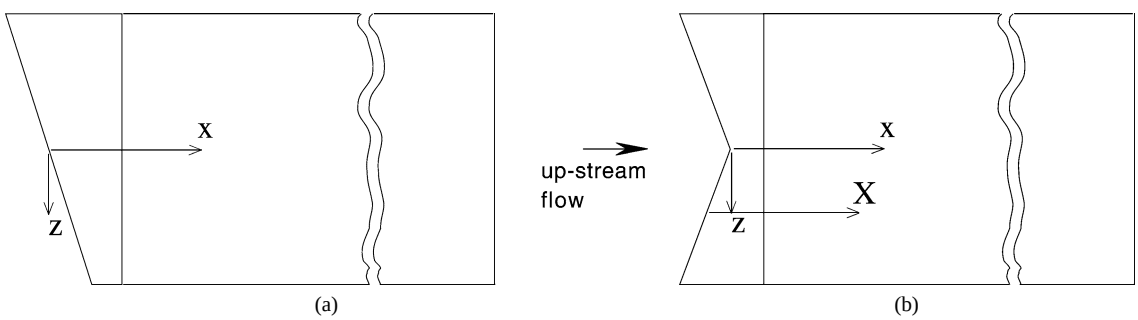

Fig. 1. Plan view of plate, showing leading-edge pieces. (a) Singly swept, (b) doubly swept.

The reference velocity,16.0 m/s, was measured in free stream flow upstream of the plate's field of influence. The free-stream mean flow was uniform to better than ±1% and the turbulence intensity less than 0.2%. The streamwise pressure gradient was measured using static pressure tappings in the roof and in the instrumentation plugs. The parameter $(\nu/\rho u_\tau^3)\,\mathrm{d}p/\mathrm{d}x$ was about 5×10^{-4} and is small enough to neglect in terms of its effect on turbulence structure of a standard boundary layer.

In the initial studies the sweep angles were 10° and ±10° as these had been employed by Hardman [17] in his study of a three-dimensional separation bubble formed in a similar way. However, after some preliminary measurements, the larger sweep was chosen to give a stronger degree of three-dimensionality. This larger angle had been used in the previous studies of Hancock and McCluskey [11] and Hancock [18]. Checks were made to ensure symmetry of the flow. Although there is no automatic reason that the flow should be symmetric simply because the flow boundaries are symmetric no evidence has suggested that this type of flow is not in principle symmetric. Symmetry is a convenient feature.

3. Results

Before presenting the results it is necessary to mention the spatial co-ordinate systems. The primary system employed here is with the streamwise distance x measured from the separation line on the plate centre line (i.e., the apex of the 'V' of the leading edge), and the lateral distance, Z, taken from this line. A second system is to take the streamwise distance X from the separation line at some perpendicular distance, Z, from the centre line – see Fig. 1(b). The third is to take distances x' and z' perpendicular and parallel to the separation line. The latter is particularly relevant to spanwise-invariant flows, since by definition, $\partial/\partial z' = 0$, though the second system is also relevant to these flows in that any quantity will be necessarily constant at constant X (as for instance X_r). y is perpendicular to and zero on the plate surface.

Other than some contour plots measurements will be presented from three planes: (i) the centre-line plane, (ii) the plane at $Z = 100$ mm $(= 2.08X_r)$ or (iii) a plane in the spanwise-invariant flow formed downstream of the singly swept separation line. The flow in the plane at $Z = 100$ mm is nominally in the spanwise-invariant region and should be no different from that in (iii). However, it turned out that the overall flow width was not really quite wide enough for there to have been side regions that were fully independent of both the central region and the effect of the wind tunnel side walls. There is no evidence to suggest that this lack of width had any significant effect on the central region except necessarily near its 'border' with the nominally invariant side regions, where the effects were small.

In order to make straightforward comparison between the general flow in the central region and the spanwise invariant flow, the normalising scale used here, unless stated otherwise, is the streamwise distance to the attachment line in the spanwise-invariant zone (and denoted by X_r, as noted earlier). This scale is preferable to that of the plate thickness in that it is a physical scale associated with the separated flow. On the centre line attachment (as measured by the two-tube probe) occurred at $x = 54$ mm.

3.1. Mean flow

Mean velocity profiles on $Z = 0$ are shown in Fig. 2 in inner-layer co-ordinates and can be compared with those for the spanwise-invariant flow in Fig. 3, where the four stations in each case correspond to the stations of the pulsed-wire measurements of wall shear stress. Note that the streamwise intervals do not correspond directly because of the leading pieces used to generate the three-dimensional flows, as outlined in Section 2. As seen in earlier studies the profiles, while showing regions of logarithmic behaviour, do not conform to the standard log law for some distance downstream. The characteristic 'dip' in the outer flow is much more pronounced in the central region. By about $8X_r$ a standard logarithmic behaviour has been established, though a dip is still present at $23X_r$, long after it has disappeared in the spanwise-invariant flow.

Contour plots of mean velocity are given in Fig. 4, where the vertical scale is exaggerated. These show a very clear 'bulge' whose shape stays much the same, with strikingly steep sides, and in about fixed proportion to the boundary layers in the side region. The downward slopes of the contours in the side regions are largely because the Z-axis is perpendicular to the centre-line, and not parallel to the leading edge. Fig. 6(a) shows the boundary layer thickness, δ, at $Z = 0$ and 100 mm, where it can be seen that they remain in about the same proportion to each other, by about a factor of 2.8. δ is defined as the point where $U = 0.99U_e$, where U_e is the local free-stream velocity. Defining the height and width of the bulge in terms of the contour at which $U = 0.99U_e$, as illustrated in Fig. 5, leads to the height and width shown in Fig. 6(b). It is striking that all these measures vary in almost constant proportion rather than, as might be supposed, mixing causing the bulge to diffuse more rapidly than the growth of the (side region) boundary layer. On this basis the presence and relative scale of the bulge persists indefinitely, implying at least in this respect the history of the separated flow is not lost. This constancy of shape also implies constancy of proportion of mean strain rates. In that the mean velocity field of the bulge is rather like a 'half-wake' it is tempting to compare its development with that of the classical far wake. From, for example, Townsend [19], an axisymmetric wake grows in width at a rate of $x^{1/3}$; the full lines in Fig. 6(b) show that bulge does indeed follow a very comparable behaviour. However, the velocity

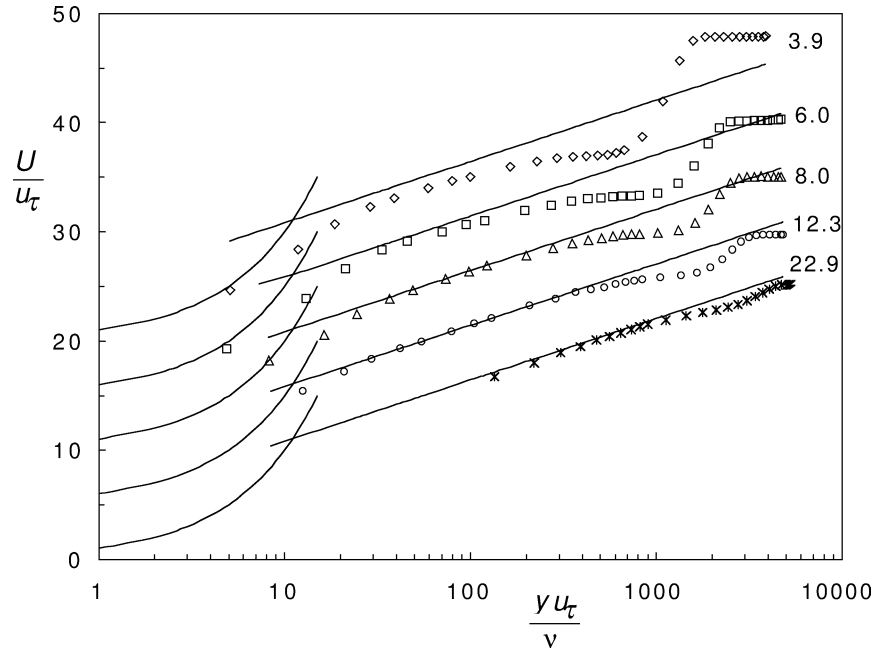

Fig. 2. Mean velocity profiles on $Z = 0$. Numbers denote x/X_r. Offsets in vertical axis: 5.

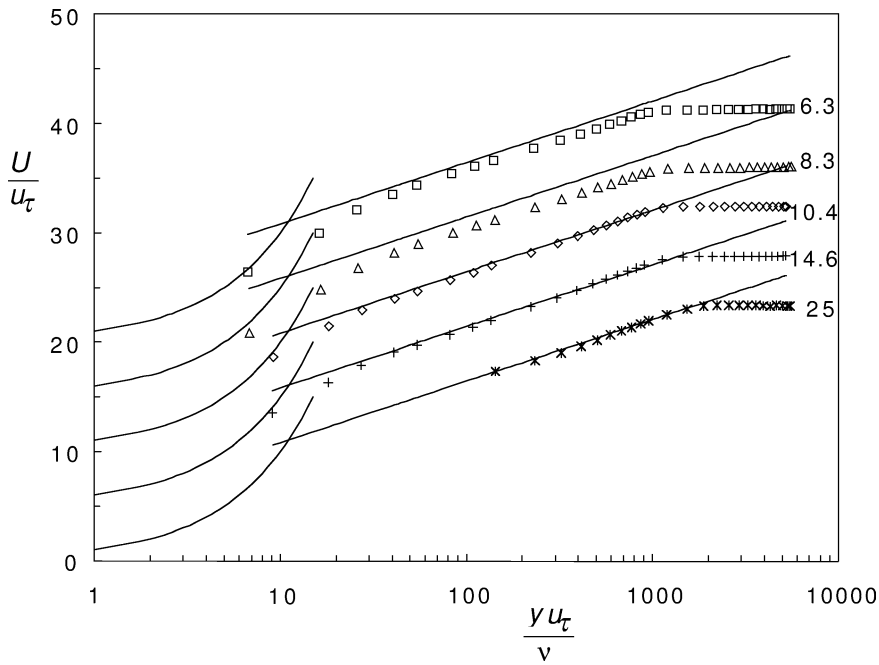

Fig. 3. Mean velocity profiles in spanwise-invariant flow. Numbers denote x/X_r. Offsets in vertical axis: 5.

deficit (not shown here) does not follow the corresponding development of $x^{-1/3}$, perhaps because the plateau in U does in fact cease after about x/X_r of 12. Nonetheless, the concept of the bulge behaving like a wake in some respects may be a useful one. Another aspect of the mean velocity profile (Fig. 2) is that inside the plateau it is quite like that of Fig. 3 – i.e., like a boundary layer, albeit at a lower free stream velocity and Reynolds number.

The vertical mean velocity, V, is everywhere much smaller than U_e and in the range where it is well known to be inaccurate (from x-wire anemometry), and is therefore not shown. For instance, slight probe alignment errors of about 1° and slight

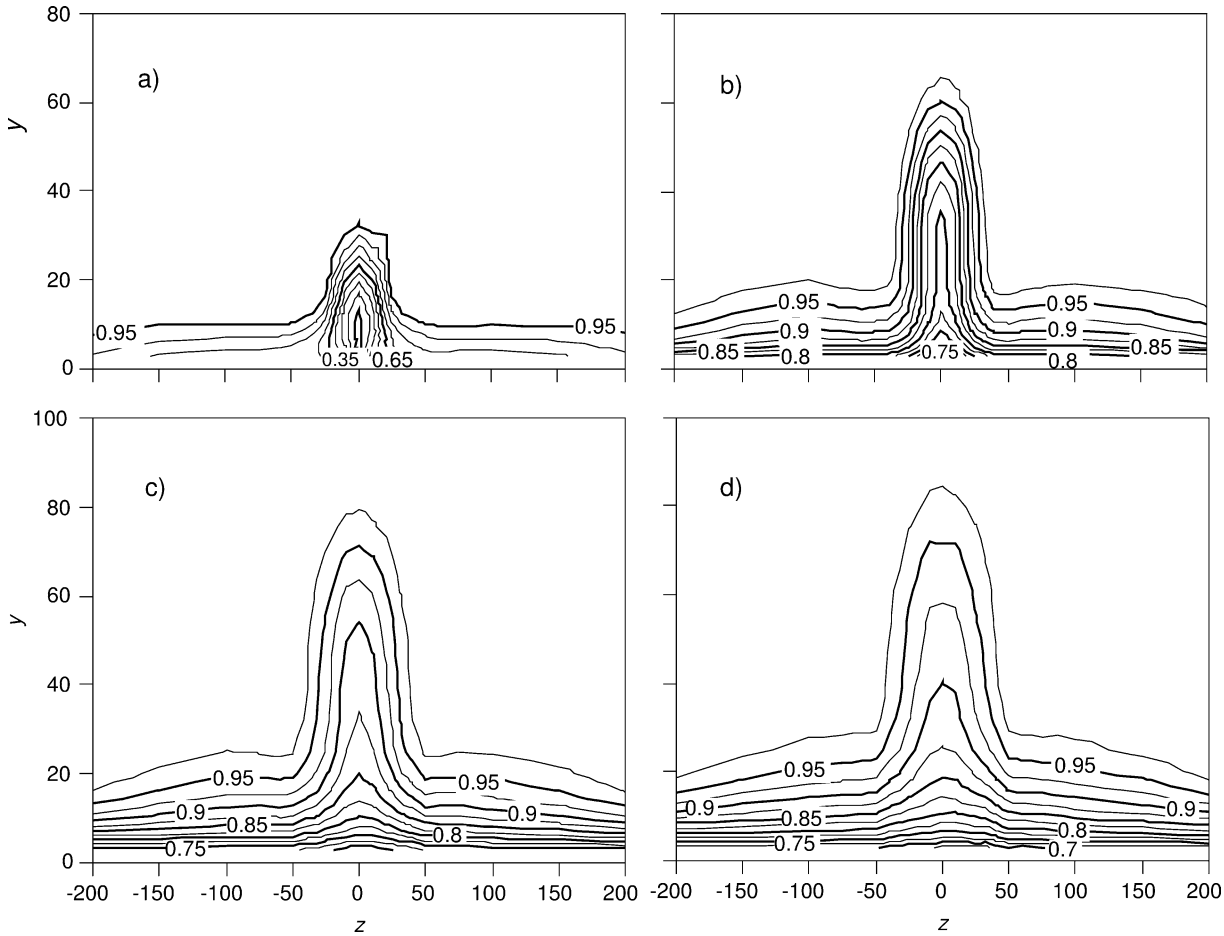

Fig. 4. Mean velocity contours. (a) $x/X_r = 2.1$; (b) 8.3; (c) 16.7; (d) 22.9.

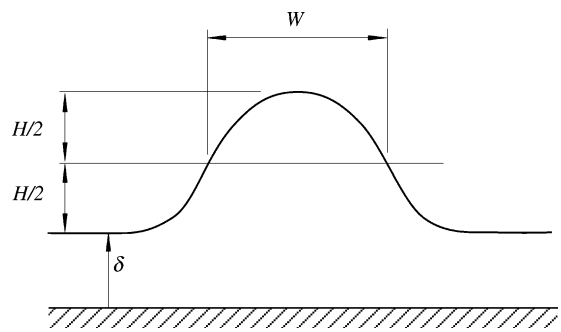

Fig. 5. Definitions of bulge height, H, and width, W.

differential drift in calibration give errors comparable with the measured levels. Essentially, the vertical mean motion is weak, typical of unperturbed boundary layer flows. The lateral mean velocity, W, was within $0.01U_e$ in the free-stream before corrections for alignment angle errors of about 0.5° where made, using the local free-stream flow to give a reference flow direction. Fig. 7 shows W/U_e for the spanwise invariant flow and at $Z = 100$ mm. W/U_e is slightly stronger at $Z = 100$ mm, and this higher level is probably caused by residual influence of the side-wall boundary layers, as mentioned earlier. Differences in flow direction are less than 1° and are largest near the surface, consistent with earlier observations of residual end effects (Hancock [18]). Fig. 8 shows pulsed-wire measurements of wall shear stress, normalised by local free-stream conditions, on $Z = 0$, in the spanwise-invariant flow, and also in the unswept flow, where the measurements for the latter two cases concur

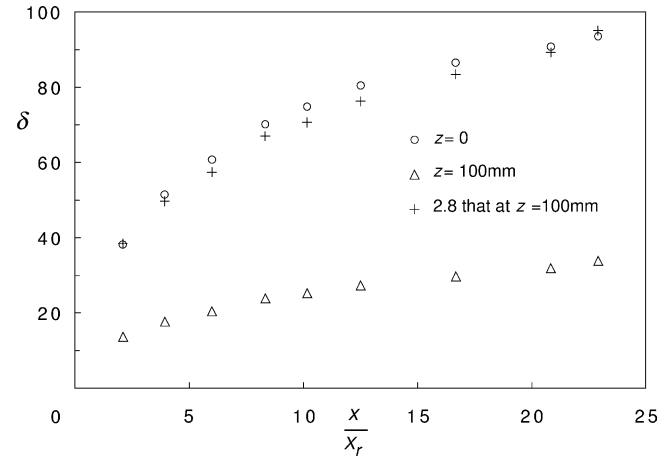

(a)

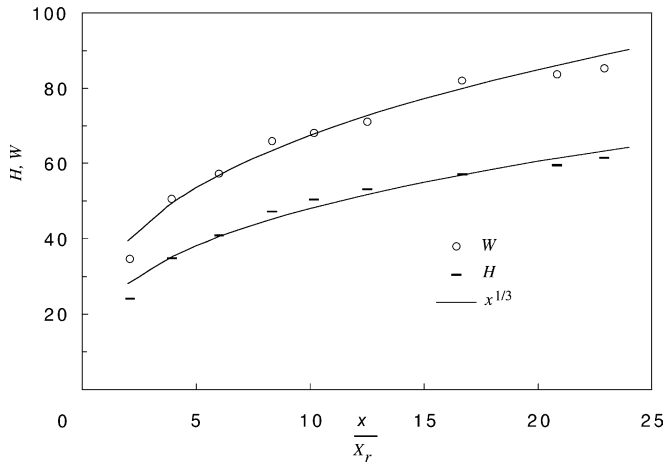

(b)

Fig. 6. (a) Boundary layer thickness on $Z = 0$ and 100 mm. (b) Bulge height and width.

very closely, providing an example of how these two flows differ only in relatively small ways. This figure also shows the shear stress inferred from fitting the velocity profile to the standard logarithmic law.

3.2. Turbulence quantities

The four non-zero Reynolds stresses on the centre plane – $\overline{uw}$ and $\overline{vw}$ are of course zero on a plane of symmetry – are shown in Fig. 9, in inner layer and outer layer co-ordinates. These figures also show profiles for a canonical boundary layer, taken from Erm and Joubert [20], also used by CE. Measurements made in a standard boundary layer on the present plate showed very close agreement with those of Erm and Joubert. These profiles are very different from their counterparts in a spanwise-invariant flow, shown in Fig. 10, the levels in the outer layer being very much higher. Not surprisingly, the outer peak in u^2 corresponds to the high gradient in $\mathrm{d}U/\mathrm{d}y$ outside the dip in the mean velocity profile. It is striking that $\overline{u^2}/u_\tau^2$ fairly quickly falls towards the standard inner-layer form even where the peak level further out is still very large compared to that in the canonical flow. The outer peak in $\overline{u^2}$ has not fallen to the level of the inner layer peak until about $7X_r$. In outer-layer scaling $\overline{u^2}$ falls well below the standard level in the inner part (at, say, $y/\delta = 0.2$) and shows no sign of returning by the last station at $23X_r$, whereas in the outer part (at, say, $y/\delta = 0.8$) it has yet to reach the standard level, if ever it does. As noted above, this higher level is of course associated with the gradient in U, which is not present in the spanwise-invariant flow this far downstream.

$\overline{v^2}$, shown in Fig. 9 (c) and (d), is very much larger than it is in the canonical flow or in the spanwise-invariant flow, given in Fig. 10 (c) and (d), and this is also true of $\overline{w^2}$ and $-\overline{uv}$. In the linear plot of Fig. 9(d), $\overline{v^2}$ can be seen to decrease sharply as the

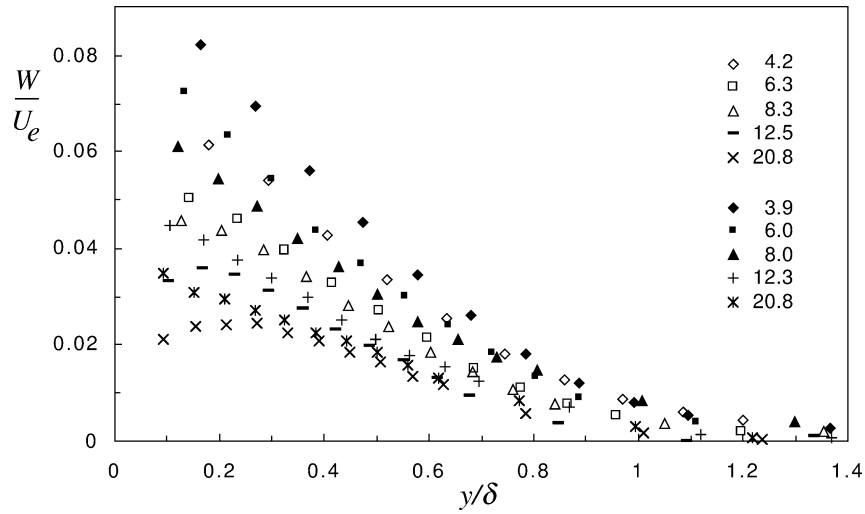

Fig. 7. Cross-flow velocity W. Open/uncrossed symbols: spanwise-invariant flow. Closed/crossed symbols: $Z = 100$ mm.

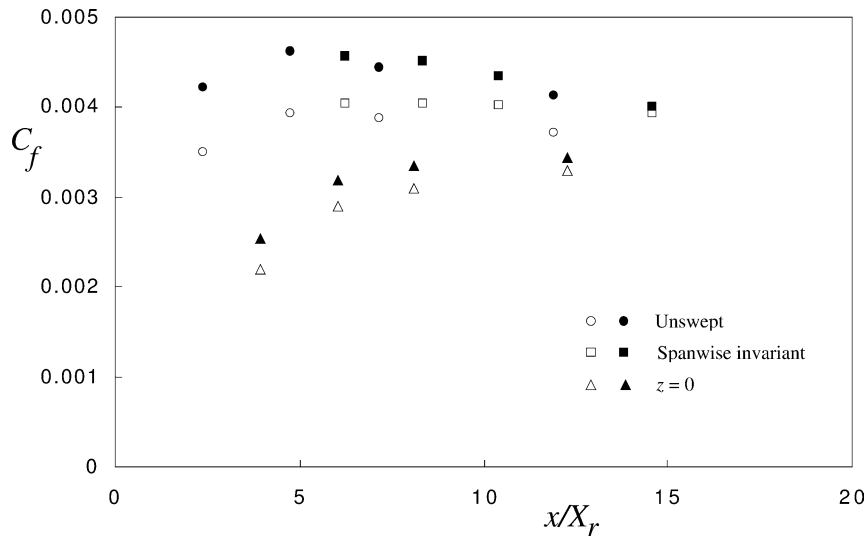

Fig. 8. Streamwise wall shear stress coefficient. Closed symbols: pulsed-wire; open symbols: log-law fit.

wall is approached, as is to be expected on the basis that the outer layer structures, as well as inner layer structures, must meet the inertial condition that v must be zero at the surface. (See, for example, Thomas and Hancock [21], Aronson et al. [22].) This implies that the scale and the effects of the outer layer structures are large enough to be felt at the wall, and it is even more curious that $\overline{u^2}$ more rapidly conforms to the inner layer canonical form. At the last station, $23X_r$, $\overline{v^2}/u_\tau^2$ has fallen in the inner region to that of the standard layer, though the level in the outer layer is still significantly higher.

$\overline{w^2}$ is also much higher than in a standard boundary layer, and much higher than in the spanwise invariant region, as shown in Figs. 9 (e) and (f) and 10 (e) and (f), respectively. It is surprising that $\overline{w^2}$ behaves quite differently from $\overline{u^2}$. Only at the last station, $23X_r$, has it almost reached the standard level in the inner layer, and this is true both on the centre line, where it starts at a much higher level, and in the spanwise-invariant flow. In outer-layer co-ordinates, on $Z = 0$, $\overline{w^2}$ like $\overline{v^2}$ has not fallen to the level of the standard boundary layer by the last station, whereas both have fallen below the standard level by this station in the spanwise-invariant flow.

The behaviour of $-\overline{uv}$ is dramatically different on the centre-plane from that in the invariant region, as can be seen by comparing Fig. 9 (g) and (h) with Fig. 10 (g) and (h). In the invariant region the shear stress profiles are mostly below the standard profile, but on the centre plane $-\overline{uv}/u_\tau^2$ is very much larger than 1 in the outer part of the flow in the neighbourhood

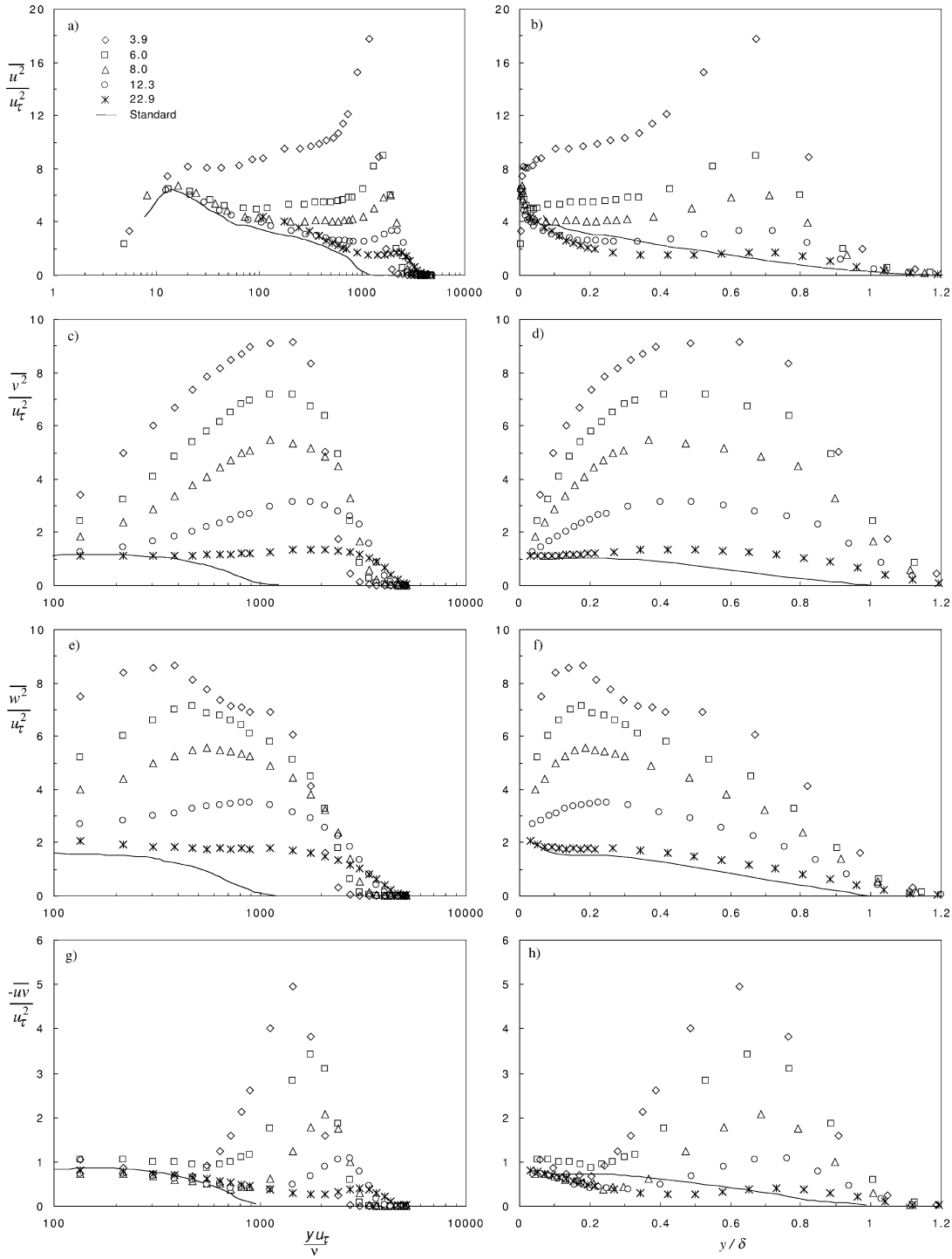

Fig. 9. Reynolds stresses on $Z = 0$. (a), (b) $\overline{u^2}$; (c), (d) $\overline{v^2}$; (e), (f) $\overline{w^2}$; (g), (h) $-\overline{uv}$. x/X_r as denoted in (a).

of the large gradient in U. At the first station $-\overline{uv}/U_e^2$ is comparable with (though less than) the level in a mixing layer. The manner in which $-\overline{uv}$ decreases with decreasing $u_\tau y/\nu$, and then follows relatively closely to the standard level for smaller $u_\tau y/\nu$, is very distinctive. A not dissimilar behaviour was observed by Song et al. [6]. The behaviour of $\overline{u^2}$ is somewhat similar

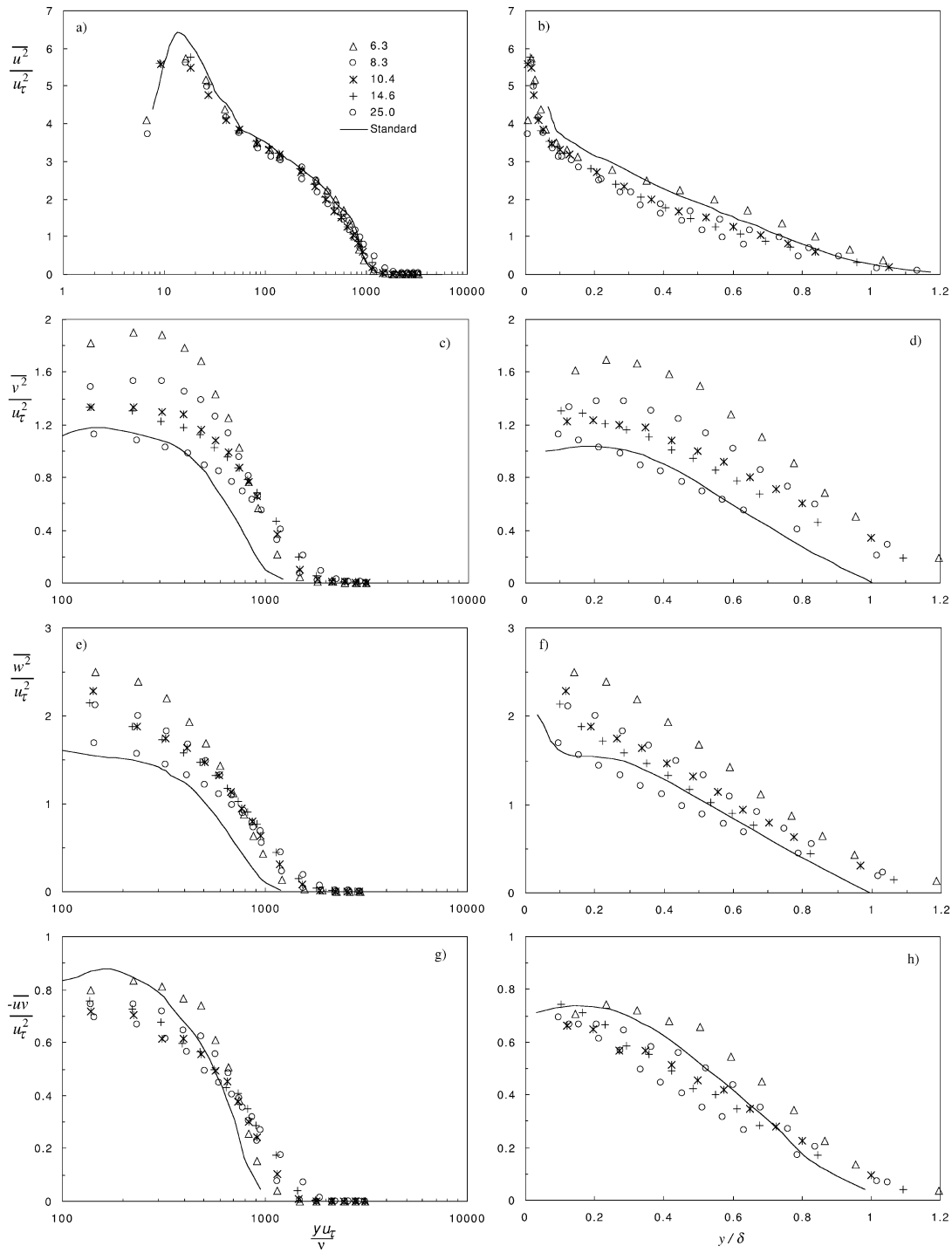

Fig. 10. Reynolds stresses in spanwise-invariant flow. (a), (b) $\overline{u^2}$; (c), (d) $\overline{v^2}$; (e), (f) $\overline{w^2}$; (g), (h) $-\overline{uv}$. x/X_r as denoted in (a).

though less pronounced and, given that the generation of $\overline{u^2}$ is $-\overline{uv}\,\mathrm{d}U/\mathrm{d}y$, profiles of U, $\overline{u^2}$ and $-\overline{uv}$ that are all fairly close to the standard levels is at least broadly self-consistent. In outer-layer co-ordinates $-\overline{uv}$ behaves much as $\overline{u^2}$ at the later stations.

The peaks in $\overline{u^2}$ and $-\overline{uv}$ occur at about the same height from the surface, at about $y/\delta = 0.7$, while the peak in $\overline{v^2}$ is at about 0.5 and the peak in $\overline{w^2}$ at about 0.2. It is noteworthy that the peak of $\overline{w^2}$ is close in level to that of $\overline{u^2}$ at the same height, and to

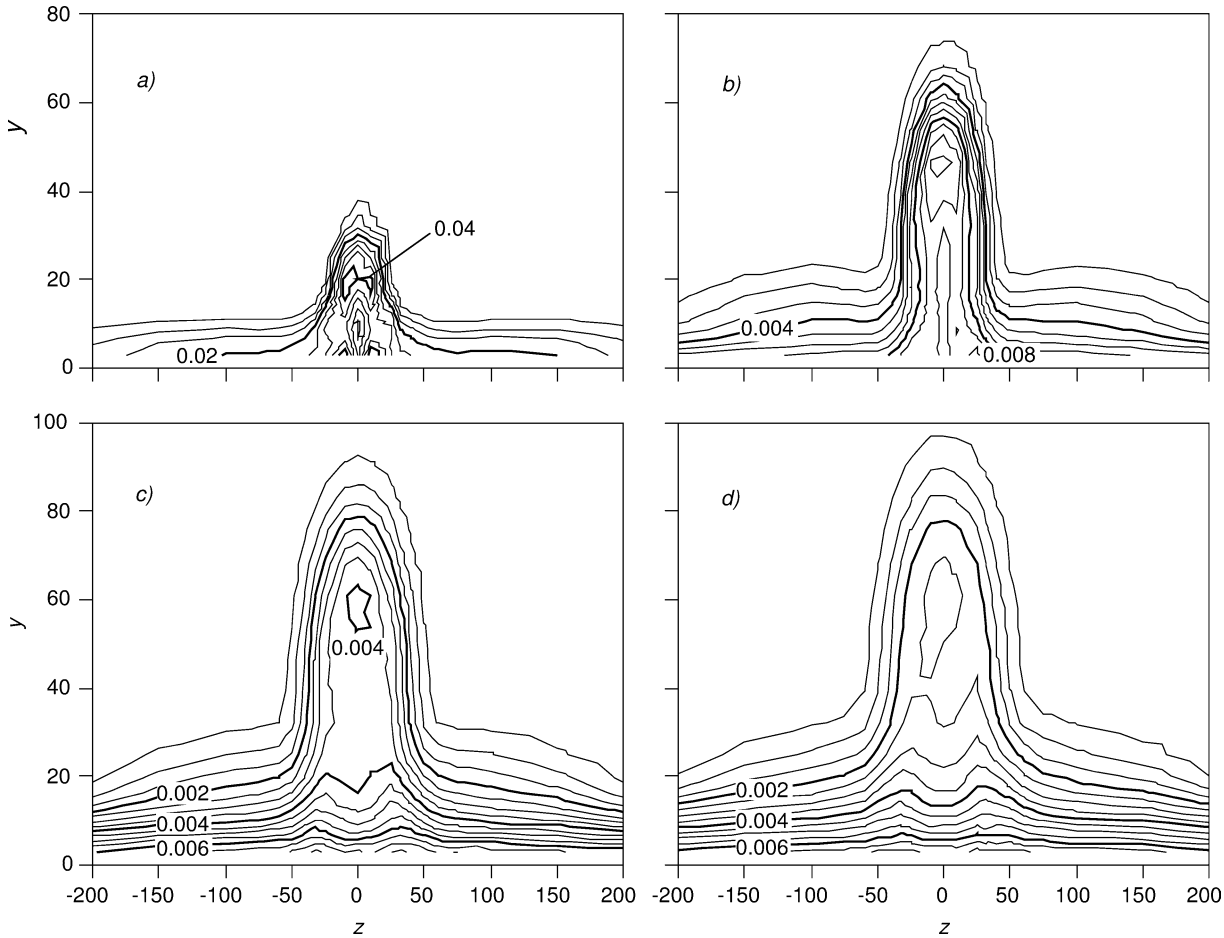

Fig. 11. Contours of $\overline{u^2}/U_e^2$. (a) $x/X_r = 2.1$; (b) 8.3; (c) 16.7; (d) 22.9.

the peak level of $\overline{v^2}$ further out. Arguably, in that $\overline{v^2}$ is large, at, say, $y/\delta = 0.2$, it is not strictly within the original concept to regard the high level of $\overline{u^2}$ and $\overline{w^2}$ (but an almost unchanged level of $-\overline{uv}$) as in-active motion – 'non-shear-stress-containing' motion might be a better term.

Examples of contours of Reynolds stresses are given in Figs. 11 and 12. Like the mean velocity contours these also show a bulge with strikingly steep sides, and an overall shape that changes very slowly with x. In detail, the stresses are not in constant proportion to each other, as can be seen for instance from the ratio of $-\overline{uv}/\overline{q^2}$ shown in Fig. 13(a), where $\overline{q^2} = \overline{u^2} + \overline{v^2} + \overline{w^2}$, and from Figs. 14(a) and 15(a). Figs. 13(b), 14(b) and 15(b) show the same ratios for the spanwise-invariant flow. Within the bulge $-\overline{uv}/\overline{q^2}$ is much less than it is in the standard boundary layer, except in the outer edge, where the level is much as in a boundary layer, though this may be fortuitous. In Figs. 13(b) and 14(b) the data are less scattered than the measurement of CE and more like the shape and level seen when free-stream turbulence is present (Hancock [23] where the profiles of $-\overline{uv}/\overline{q^2}$ are closely proportional to the profiles of $-\overline{uv}/(\overline{u^2}\,\overline{v^2})^{1/2}$ given in Hancock and Bradshaw [4]). The low levels of $-\overline{uv}/\overline{q^2}$ on the centre line are related of course to low levels of $\overline{uv}$ and, it is supposed, to the plateau in the mean velocity profile, in much the same way as $-\overline{uv}/\overline{q^2}$ is low above the outer edge of a shear layer.

All the contour profiles show degrees of imperfect symmetry, and this is most noticeable in those of $\overline{uv}$ and $\overline{uw}$, which are also the smallest in magnitude of the five stresses, the last being the smaller of these two. (Fig. 12 is typical.) It is possibly that some of this asymmetry is a genuine residual asymmetry originating in the separated region. Some is likely to be measurement error. There is no clear indication that the flow is inherently slightly asymmetric.

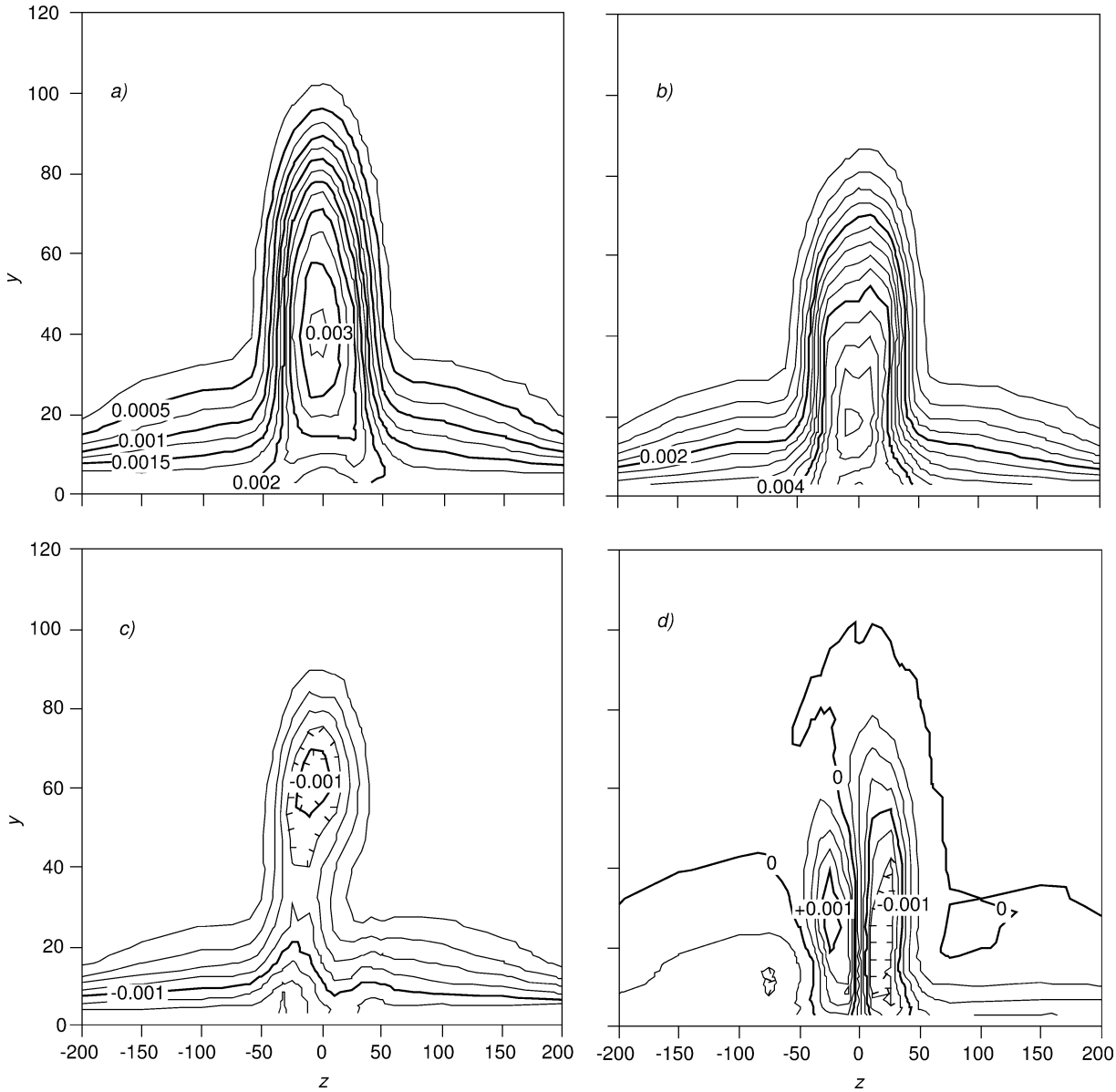

Fig. 12. Contours of $\overline{v^2}$, $\overline{w^2}$, $\overline{uv}$ and $\overline{uw}$ at $x/X_r = 16.7$, normalised by U_e^2. (a) $\overline{v^2}$; (b) $\overline{w^2}$; (c) $\overline{uv}$; (d) $\overline{uw}$.

4. Discussion and concluding comments

The flow downstream of the present three-dimensional flow is different in fundamental ways from that downstream of two-dimensional flow, whether it is a two-dimensional co-planar flow as in the studies of CE and Song et al., for example, or a two-dimensional but nonco-planar flow as in that generated by a swept separation line (e.g., [10]). The converging flow generated within the separated region leads to an up-flow and a bulge in and immediately downstream of this region, a bulge which is very persistent, perhaps permanent, or requiring a distance an order of magnitude longer before it would 'disappear' into the background of the adjacent boundary layers. Arguably, the development of the bulge could be assessed in terms of a length scale that takes into account its greater thickness, such as a length scale of, say, $2.8X_r$, but even on this basis the dip in the mean velocity profile is significantly slower to disappear. Any streamwise vortex-like rotating motions within the bulge are weak, with a weak common up flow. The persistence of a plateau in the mean velocity and its decreasing deficit with respect to

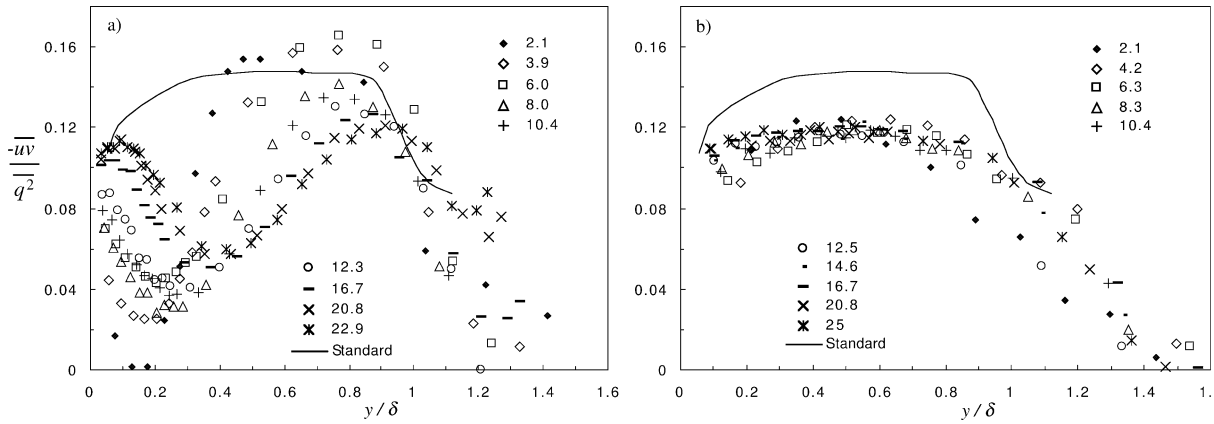

Fig. 13. Profiles of $-\overline{uv}/\overline{q^2}$, (a) on $Z = 0$, (b) spanwise-invariant flow.

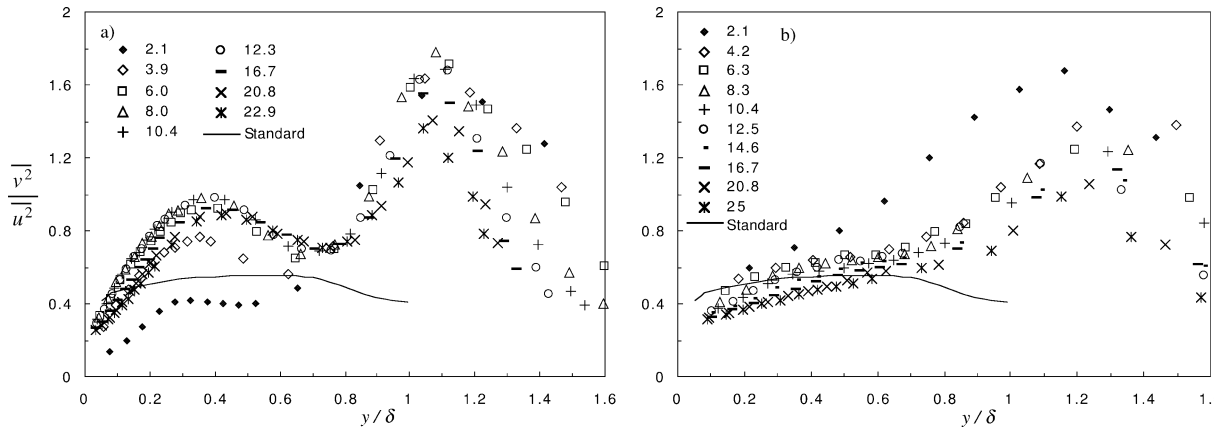

Fig. 14. Profiles of $\overline{v^2}/\overline{u^2}$, (a) on $Z = 0$, (b) spanwise-invariant flow.

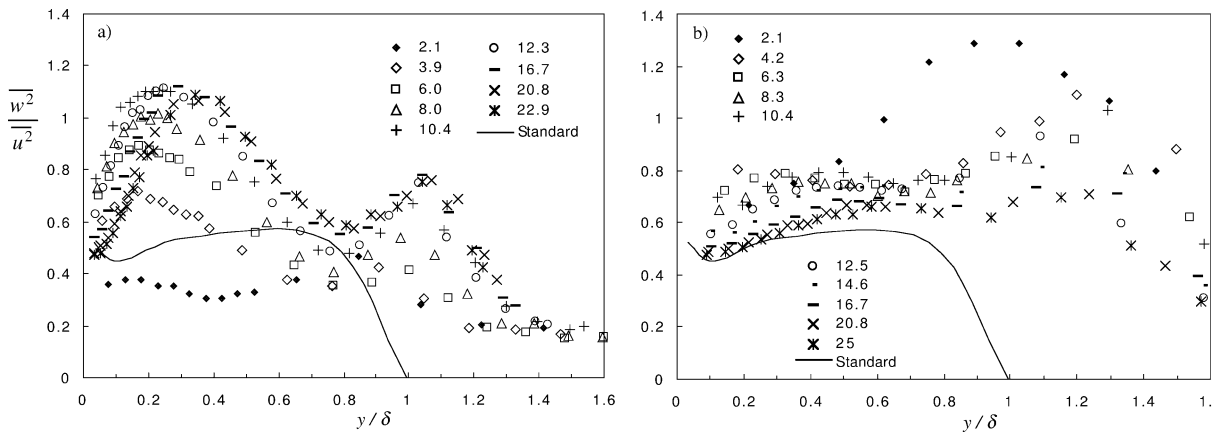

Fig. 15. Profiles of $\overline{w^2}/\overline{u^2}$, (a) on $Z = 0$, (b) spanwise-invariant flow.

the free-stream velocity is one of the features that give the bulge a wake-line characteristic, as is its growth rate of height and width following an approximately $x^{1/3}$ form, characteristic of axi-symmetric wakes.

Beneath the bulge $\overline{w^2}$ is the slowest to develop toward that of the standard boundary layer. Surprisingly, $\overline{u^2}$ and more so $-\overline{uv}$ fall quickly to follow fairly closely an inner-layer-like scaling, even though these quantities are very much larger in the

overlying bulge than in the outer part of a standard boundary layer. A comparable behaviour is seen in the inner layer of the spanwise invariant flow even though there is no strong turbulence in the outer flow. This behaviour of $\overline{u^2}$ and $-\overline{uv}$ supports the stress-equilibrium layer idea of Song et al. though $\overline{v^2}$, here, does not conform nearly as readily as in their measurements. They did not measure $\overline{w^2}$ or $\overline{uw}$. In some of the cases of free-stream turbulence acting on an otherwise standard boundary layer Hancock and Bradshaw [4] found that the fractional increase in $\overline{w^2}$ was larger than that in $\overline{u^2}$, rather as here. Thus, as regards the development of the inner layer, it does develop towards that of the canonical layer more quickly than the outer layer, except in so far as the outer flow is like free-stream turbulence above an otherwise standard inner layer, imposing non-shear-stress-containing (as distinct from inactive) motions. In the inner part of the layer $\overline{u^2}$ and $-\overline{uv}$ undershoot the standard, but $\overline{v^2}$ and $\overline{w^2}$ either reach the canonical state monotonically, or take even longer non-monotonically. In the outer part, i.e., in the bulge part, none of the stresses had reached the standard levels by the last station $(23X_r)$.

There are some qualitative similarities between the present flow and that of a boundary layer flow with a pair of imbedded streamwise vorticies generating an up-flow, as studied for instance by Mehta and Bradshaw [12]. (Vortices of the opposite sense generate a very different flow – a down flow and a dip, rather than a bulge – and the vortices move apart. See, for example, Pauley and Eaton [24].) The up-flow leads to a mushroom-shaped bulge that is roughly in the same proportion to that here, the mushroom shape arising from the much stronger vorticity. There is also a reduction in shear stress in relation to the direct stresses, not too different from that here.

As noted earlier, the wake-like structure, with its characteristics of the far wake, has its origins in the separated flow. The classical wake arises from either attached boundary layers merging at a trailing edge or from the separated flow region downstream of a bluff body. In the former case, the wake develops from a growing inner layer in the near-wake region. Prediction methods for this type of wake therefore need to represent the effects of the sudden removal of the wall shear stress, the changes taking place at scales of order of the inner length scales, the outer flow changing much more slowly. The wake of a bluff body is fundamentally different in that the development of the near wake involves changes at all length scales up to the largest, which are of order the wake width. The present flow is much more like the latter than it is the former, and accurate prediction of its early formation will depend upon accurate prediction of the separated flow itself.

Although the present flow is an idealised one it is expected that more general separated flows in which there is a lateral convergence of the flow within the separated region will exhibit similar characteristics to those observed here. An asymmetric region of converging separated flow is likely to lead to an asymmetric bulge, but the absence of streamwise vorticies is likely to remain (since their absence in the present flow is not a consequence of symmetry as such). This being so, physical models that accurately represent the processes in this special case are likely to be successful in the more general flow than would otherwise be the case. It would seem that prediction should be easier than for flows in which there are imbedded streamwise vorticies in that there is no significant rotation of the structures [12].

A separated region, converse to that here, within which the flow diverges rather than converges, as can be realised by the separation lines forming an upstream-facing V, would (from continuity considerations) lead to a ‘dip’ rather than a bulge, and perhaps a much lower level of outer layer turbulence than in a two-dimensional flow. As to whether this dip would be equally persistent, and for instance exhibit equally characteristic steep sides as seen in the bulge, is a matter for further investigation, of course.

Acknowledgements

This project was supported by a School of Engineering scholarship (for C. Cao) and by funds from the Fluids Research Centre. The authors also wish to express their grateful thanks to Mr T. Lawton and Mr A. Wells for the design and construction of the probe traversing system and to Dr P. Hayden for assistance with the data acquisition software.

References

[1] I.P. Castro, E. Epik, Boundary layer development after a separated region, J. Fluid Mech. 374 (1998) 91–116.
[2] H.H. Fernholz, Near-wall phenomena in turbulent separated flows, Acta Mech. Suppl. 4 (1994) 57–67.
[3] P. Bradshaw, Turbulence: the chief outstanding difficulty of our subject, Exp. in Fluids 16 (1994) 203–216.
[4] P.E. Hancock, P. Bradshaw, Turbulence structure of a boundary layer beneath a turbulent free stream, J. Fluid Mech. 205 (1989) 45–76.
[5] P. Bradshaw, F.Y.F. Wong, The reattachment and relaxation of a turbulent shear layer, J. Fluid Mech. 52 (1972) 113–135.
[6] S. Song, D.B. DeGraaff, J.K. Eaton, Experimental study of a separating, reattacing, and redeveloping flow over a smoothly contoures ramp, Int. J. Heat Fluid Flow 21 (2000) 512–519.
[7] D.B. DeGraaff, J.K. Eaton, Reynolds number scaling of the turbulent boundary layer on a flat plate and on swept and unswept bumps, Report TSD-118, Stanford University, 1999.

[8] M. Kalter, H.H. Fernholz, The reduction and elimination of a closed separation region by free-stream turbulence, J. Fluid Mech. 446 (2001) 271–308.
[9] J.R. Hardman, P.E. Hancock, The near-wall layer beneath a moderately converging three-dimensional turbulent separated and reattaching flow, Eur. J. Mech. B Fluids 19 (2000) 653–672.
[10] H.J. Kaltenbach, The swept backward-facing step with an upstream turbulent boundary layer, in: I.P. Castro, P.E. Hancock, T.G. Thomas (Eds.), Adv. in Turbulence,Y|X, CIMNE, 2002, pp. 73–76.
[11] P.E. Hancock, F.M. McCluskey, Spanwise-invariant three-dimensional separated flow, J. Exp. Thermal Fluid Sci. 14 (1997) 25–34.
[12] R.D. Mehta, P. Bradshaw, Longitudinal vortices imbedded in turbulent boundary layers. Part 2. Vortex pair with 'common flow' upwards, J. Fluid Mech. 188 (1988) 529–546.
[13] I.P. Castro, J.E. Fackrell, A note on two-dimensional fence flows, with emphasis on wall constraint, J. Ind. Aerodynamics 3 (1978) 1–20.
[14] N.J. Cherry, R. Hillier, M.E.M.P. Latour, Unsteady measurements in a separated and reattaching flow, J. Fluid Mech. 144 (1984) 13–46.
[15] P. Bradshaw, An Introduction to Turbulence and its Measurement, Pergamon, 1971.
[16] V.C. Patel, Calibration of the Preston tube and limitations on its use in pressure gradients, J. Fluid Mech. 23 (1965) 185–208.
[17] J.R. Hardman, Moderately three-dimensional separated and reattaching turbulent flow. Ph.D. thesis, University of Surrey, 1998.
[18] P.E. Hancock, Measurements of mean and fluctuating wall shear stress beneath spanwise-invariant separation bubbles, Exp. Fluids 27 (1999) 53–59.
[19] A.A. Townsend, The Structure of Turbulent Shear Flow, Cambridge University Press, 1976.
[20] L.P. Erm, P.N. Joubert, Low-Reynolds-number turbulent boundary layers, J. Fluid Mech. 230 (1991) 1–44.
[21] N.H. Thomas, P.E. Hancock, Grid turbulence near a moving wall, J. Fluid Mech. 82 (1977) 481–496.
[22] D. Aronson, A.V. Johansson, L. Löfdahl, Shear-free turbulence near a wall, J. Fluid Mech. 338 (1997) 363–385.
[23] P. E. Hancock, The effect of free-stream turbulence on turbulent boundary layers. Ph.D. thesis, Imperial College, University of London, 1980.
[24] W.R. Pauley, J.K. Eaton, Experimental study of the development of longitudinal vortex pairs embedded in a turbulent boundary layer, AIAA J. 26 (1988) 816–823.